

Cite this: *J. Mater. Chem. C*, 2014, 2, 6743

Phosphorescent light-emitting diodes using triscarbazole/bis(oxadiazole) hosts: comparison of homopolymer blends and random and block copolymers†

Xuyang He,^a Dengke Cai,^b Dun-Yen Kang,^{‡a} Wojciech Haske,^b Yadong Zhang,^a Carlos A. Zuniga,^a Benjamin H. Wunsch,^a Stephen Barlow,^a Johannes Leisen,^a David Bucknall,^c Bernard Kippelen^{*b} and Seth R. Marder^{*b}

Examples of blends of carbazole- and bis(oxadiazole)benzene-based side-chain polymers have recently been reported to be efficient host materials for phosphorescent emitters in organic light-emitting diodes. Here, the properties and performance of a physical blend of polynorbornene homopolymers with triscarbazole and bis(oxadiazole)benzene side chains are compared to those of random and block copolymers of the corresponding triscarbazole- and bis(oxadiazole)benzene-functionalized monomers. Green-emitting devices in which the blend is used a host for Ir(ppy)₃ are significantly more efficient than those based on copolymers. Differential scanning calorimetry and solid-state NMR data show that there is no macroscale separation between the two polymers in the blend. The NMR data suggest that there are significant differences in the dimensionality and characteristic length of nanoscale domain structures in the block copolymer and the blend. Use of Ir(ppy)₃ in place of Ir(ppy)₃ leads to even more efficient light-emitting diodes, with external quantum efficiencies of up to ca. 21% (at 100 cd m⁻²).

Received 23rd May 2014
Accepted 24th June 2014

DOI: 10.1039/c4tc01079e

www.rsc.org/MaterialsC

Introduction

The emissive layers of phosphorescent organic light-emitting diodes (PHOLEDs) typically incorporate heavy-metal emitters, often iridium(III) complexes¹ diluted in a suitable host at relatively low concentration to reduce the incidence of triplet-triplet annihilation.² In general, the triplet and singlet excited-state energies of the hosts should be higher than the corresponding energies of the emitters to favor forward energy transfer to the emitter and minimize back energy transfer from the emitter to the host. In addition, it is desirable that the glass-transition temperature of the host be sufficiently high to maintain a stable morphology of the emissive layer in the solid-state device at operational temperatures.

Hosts with ambipolar charge-transporting ability are potentially advantageous over unipolar host materials in providing a broader recombination zone in the emissive layer, thereby reducing the possibility of triplet-triplet quenching.³ In some cases the use of ambipolar hosts can facilitate simpler device structures.⁴ A widely used approach to ambipolar materials is to combine electron-transporting and hole-transporting moieties⁵ either through a covalent linker – in small-molecules or as copolymers – or as a physical blend – either of small molecules, a small molecule and a polymer, or of different polymers. Carbazoles and oxadiazole derivatives are among the most widely used groups for hole- and electron-transporting host components, respectively. There are various ways to incorporate both moieties: as blends of polymeric carbazole derivatives, such as poly(*N*-vinylcarbazole) (PVK), with small-molecule or polymeric oxadiazole derivatives,^{4a,4b,4e,6} as random and block copolymers of carbazole- and oxadiazole-based monomers,⁷ and as carbazole-backbone polymers with oxadiazole pendants.⁸ Molecular hosts have also been used in which carbazole and oxadiazole moieties are connected in an either conjugated or non-conjugated manner.⁹ We have reported that physical blends of carbazole- and oxadiazole-based polymers can be used as solution-processible hosts for green-emitting iridium phosphors in efficient PHOLEDs. Devices using crosslinked poly-TPD-F as a hole-transport layer, a blend of poly(*N*-vinylcarbazole) (PVK), poly(norbornene)s with 1,3-bis(5-phenyl-1,3,4-

^aCenter for Organic Photonics and Electronics and School of Chemistry and Biochemistry, Georgia Institute of Technology, Atlanta, GA 30332-0400, USA. E-mail: seth.marder@chemistry.gatech.edu

^bCenter for Organic Photonics and Electronics and School of Electrical and Computer Engineering, USA. E-mail: bernard.kippelen@ece.gatech.edu

^cCenter for Organic Photonics and Electronics and School of Materials Science and Engineering, Georgia Institute of Technology, Atlanta, GA 30332-0245, USA

† Electronic supplementary information (ESI) available: Synthesis of monomers and of Sty₂-TCz, solid-state NMR spectra and details of spin-diffusion experiments, table of absorption/fluorescence maxima, figures showing OLED performance. See DOI: 10.1039/c4tc01079e

‡ Present address: Department of Chemical Engineering, National Taiwan University, Taipei, Taiwan.

oxadiazol-2-yl)benzene side chains (**I**), and Ir(ppy)₃ or Ir(pppy)₃ phosphors (see Fig. 1 for structures) as the emissive layer, and a vacuum-deposited BCP electron-transport layer exhibited EQEs approaching 13%.^{6c} More recently, we have also achieved similar performance using a blend of substituted polystyrenes with 3,6-bis(carbazol-9-yl)carbazole (“triscarbazole”) and 1,3-bis(5-phenyl-1,3,4-oxadiazol-2-yl)benzene side chains (**II** and **III**, Fig. 1) as the host for Ir(ppy)₃, in conjunction with hole-transport layers based on copolymers of styrene monomers substituted with triscarbazole and oxetane or benzocyclobutene crosslinkable side chains, and a BCP electron-transport layer.¹⁰ Here we directly compare the performance as a host of a related blend of polymers (poly-1/poly-2; Scheme 1) with that of random

(1-co-2) and diblock copolymers (1-b-2) and present photo-physical and solid-state NMR data that show differences between these different approaches to host materials.

Experimental section

¹H NMR and ¹³C{¹H} NMR spectra were recorded on a 400 MHz Bruker DMX spectrometer and were referenced using the residual solvent proton and carbon signals. Elemental analyses were carried out by Atlantic Microlab Inc. Mass spectra (EI) were recorded on a Micromass Autospace mass spectrometer and Applied Biosystems 4700 Proteomics Analyzer mass spectrometer. The molecular weights of the polymers were estimated in tetrahydrofuran (THF) by using gel permeation chromatography using a Waters 1515 pump, a Waters 2489 UV-vis detector, a Styragel HR 5E THF 4.6 × 300 mm column, and linear poly(styrene) standards. Differential scanning calorimetry (DSC) data were obtained using a TA DSCQ200 at a heating rate of 10 °C min⁻¹ from 40 to 300 °C under a nitrogen atmosphere. Thermogravimetric analysis (TGA) was performed on a NETZSCH STA 449C instrument at a heating rate of 20 °C min⁻¹ from 20 to 500 °C. UV-vis absorption spectra were measured on a Hewlett-Packard 8453 spectrometer. Fluorescence spectra were recorded on a Fluorolog III ISA spectrofluorimeter.

¹H spin diffusion experiments and simulations

The samples for the ¹H spin diffusion experiments were prepared from drop-casting the as-synthesized polymers dissolved in chlorobenzene with a concentration of 10 mg mL⁻¹ into a glass vial. The vials with solution were placed in a convection oven at 50 °C for 12 h followed by at 120 °C for 6 h yielding solid-state polymer samples. Solid-state samples (ca. 50 mg portions) obtained in this way were used for NMR experiments. The experiments were performed using a Bruker DSX 300 NMR spectrometer with a static H/X broadband probe. Experiments were conducted at 190 °C, at which temperature the oxadiazole domain exhibits significant large-angle molecular motions with frequencies larger than >ca. 10 kHz in comparison to the rigid triscarbazole domain according to the spin-spin relaxation results, which showed two distinct relaxation times assigned to two domains. The conduct of the spin-diffusion experiment follows closely the experimental approach as described by Mellinger *et al.*¹¹ Briefly, the magnetization of the mobile poly-1 domain is selected through the repeated application of a rf-pulse train consisting of 12 π/2-pulses (dipolar filter), which is followed by a π-pulse to align magnetization along the z-axis, a mixing time and a readout pulse followed by the detection. A good selection was achieved for n = 4 pulse trains, where individual pulses with a duration of 3.6 μs were separated by a delay of 20 μs. I_{DF}⁰, the amount of magnetization corresponding to poly-1, was determined by integration over the corresponding narrow peak. Contribution of the longitudinal relaxation T₁ were eliminated by conducting the same experiment without the dipolar filter (*i.e.* n = 0) measuring an intensity I_{DF}⁰. The (normalized) ratio I_{DF}/I_{DF}⁰ as displayed in Fig. 5 will then provide a reliable measurement of the

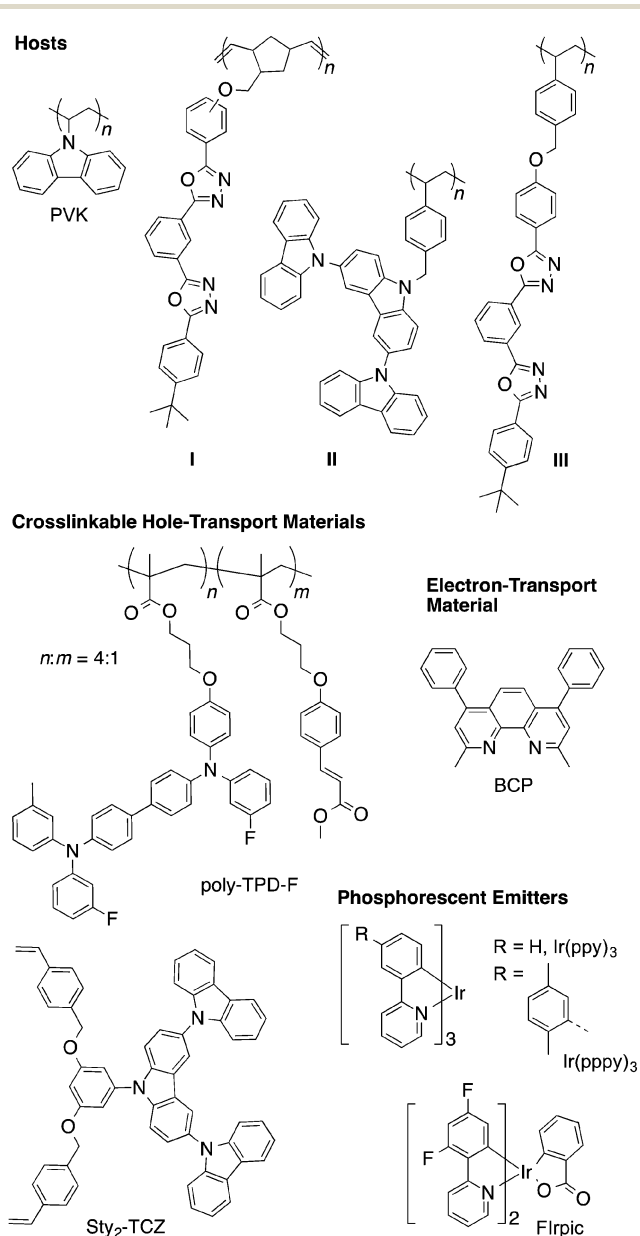
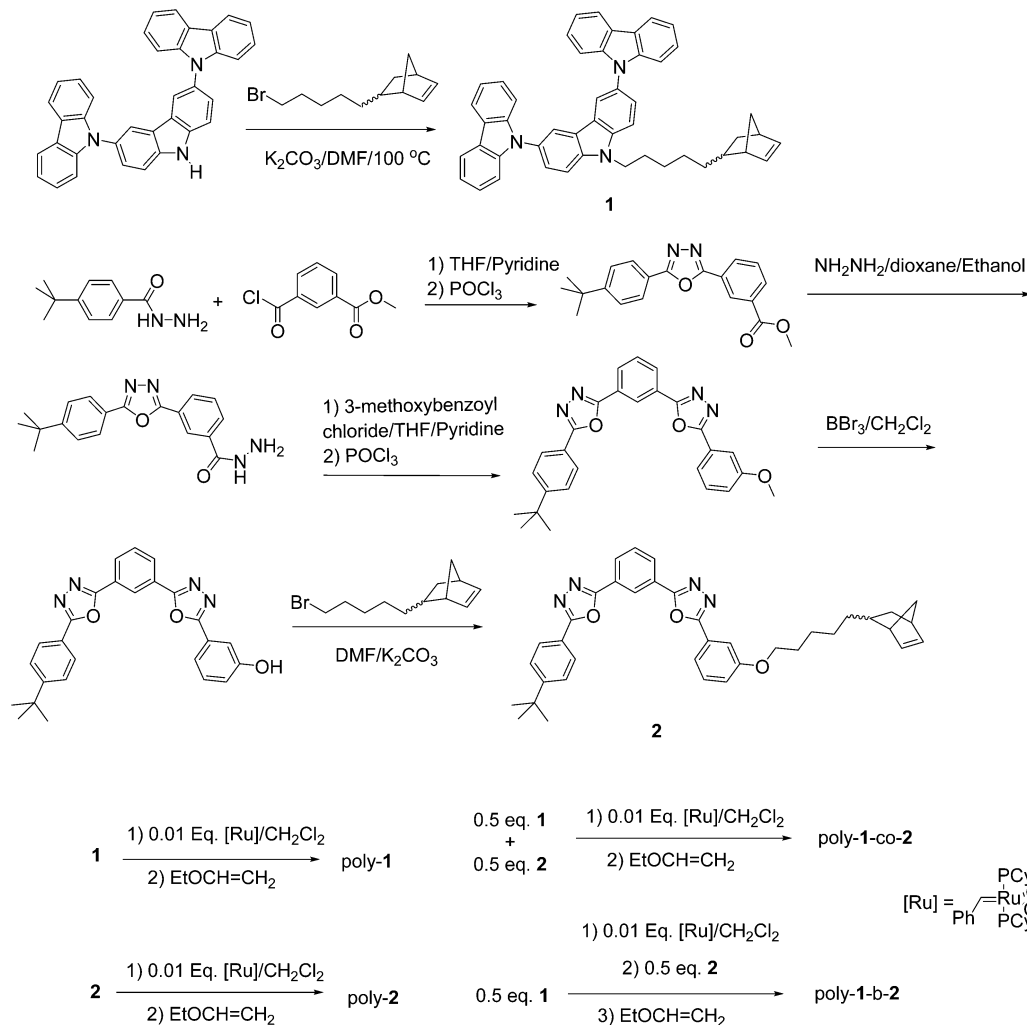


Fig. 1 Structures of some polymers previously used in blends as hosts, along with those of phosphors and transport materials discussed in this paper.



Scheme 1 Synthesis and polymerization of 1 and 2.

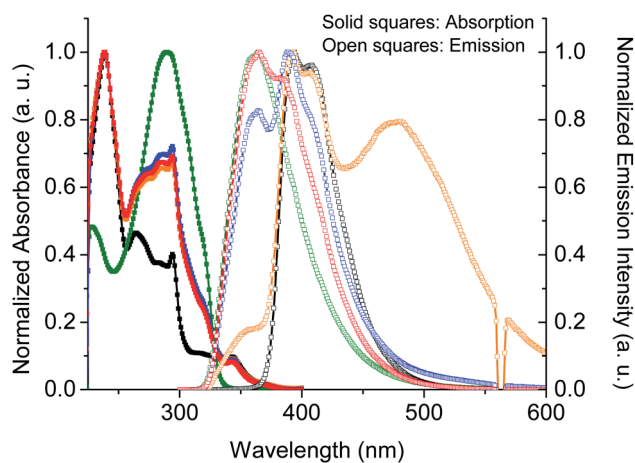


Fig. 2 Absorption (solid squares) and emission (open squares, excitation wavelength of 280 nm) spectra of poly-1 (black), poly-2 (olive), poly-1-co-2 (orange), poly-1-b-2 (blue), and 1 : 1 poly-1/poly-2 (red) in CH_2Cl_2 .

magnetization leaving the poly-1 phase through spin diffusion. Spin-diffusion coefficients were estimated from measured T_2 -relaxation constants using the calibration curves.¹¹ T_2 -relaxation data were measured using a regular spin-echo sequence. This resulted in a biexponential decay, providing the relaxation constants for both phases (details are presented in the ESI†).

The 1H spin diffusion between two domains was modeled by Fick's law of diffusion:¹²

$$\frac{\partial M}{\partial t} = -D\nabla M \quad (1)$$

where M is the normalized magnetization (a.u.), t is time (ms), and D is the spin diffusion coefficient ($nm^2 ms^{-1}$). The advantage of this approach is that it can be readily expanded for the study of more complex geometries. For the domain geometry, two line segments, two concentric squares, and two concentric cubics were regarded as the representative geometries for the one-, two-, and three-dimensional diffusion process respectively. Fick's law was applied as the governing equation for the spin diffusion with the known diffusion coefficients obtained from the spin-spin relaxation experiments. Continuous

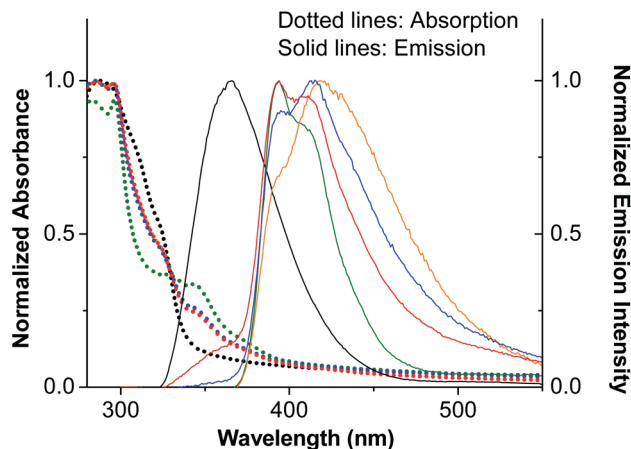


Fig. 3 Absorption (dotted lines) and emission (solid lines, excitation wavelength of 280 nm) spectra of poly-1 (olive), poly-2 (black), poly-1-co-2 (orange), poly-1-b-2 (blue), and 1 : 1 poly-1/poly-2 (red) in the solid state.

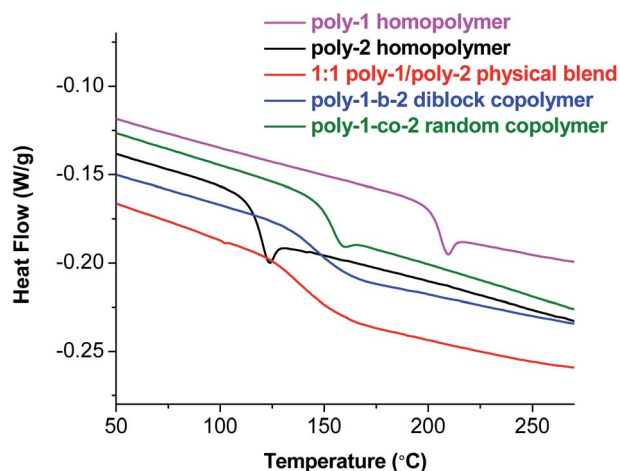


Fig. 4 1 DSC plots (exothermic up) of poly-1, poly-2, poly-1-co-2, poly-1-b-2, and 1 : 1 poly-1/poly-2 obtained at a heating rate of $10\text{ }^{\circ}\text{C min}^{-1}$.

boundary conditions were applied at the interfaces of the two domains. The normalized magnetization for the oxadiazole domain was taken as one and the triscarbazole domain was taken as zero as the initial condition. The transient spin-diffusion equation (eqn (1)) was solved for the given domain sizes numerically using the widely used software package COMSOL®. The domain-average magnetization intensity for the triscarbazole domain was then obtained from the numerical solution as a function of time and then compared with the experimental results.

OLED fabrication

Indium tin oxide (ITO)-coated glass (Colorado Concept Coatings LLC) with a sheet resistivity of $\sim 15\ \Omega\ \text{sq}^{-1}$ was used as the substrate for the OLEDs fabrication. The ITO substrates were patterned with Kapton tape and etched in acid vapor (1 : 3 by

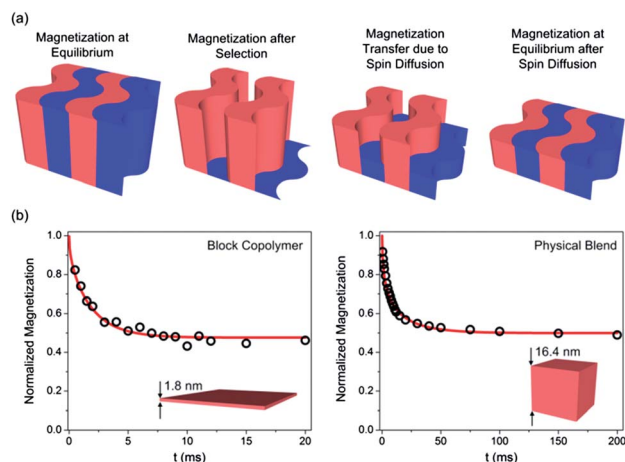


Fig. 5 (a) Illustration of the key steps in the ^1H spin diffusion process. (b) Experimental (black circle) and simulated (red curve) results of the normalized magnetization of the mobile phase (poly-2 domain) as a function of the spin diffusion time.

volume, $\text{HNO}_3 : \text{HCl}$) for 5 min at $60\text{ }^{\circ}\text{C}$. The substrates were cleaned in an ultrasonic bath of detergent water, rinsed with deionized water, and then cleaned in sequential (20 min each) ultrasonic baths of deionized water, acetone, and isopropanol. Nitrogen was used to dry the substrates after each of the last three baths. The substrates were treated with an O_2 plasma for 3 min prior to the deposition of the hole-transport material.

For the green-emitting devices 35 nm thick films of poly-TPD-F¹³ were then spin coated (60 s at 1500 rpm, acceleration $10\ 000\ \text{rpm s}^{-1}$) from a solution of poly-TPD-F (10 mg) in chloroform (1 mL, 99.8% purity, distilled and oxygenated) in a N_2 -filled glove box. After spin-coating, a rectangular strip of the layer was removed at the edge of the substrate to expose ITO and ensure electrical contact to the anode; then, the sample was dried in vacuum and transferred back into the glove-box, where it was baked for 15 min at $75\text{ }^{\circ}\text{C}$ on a hot plate, after which the hot plate was turned off. The sample was removed from the hot plate when its temperature was down to $40\text{ }^{\circ}\text{C}$. Finally the sample was exposed to $0.7\ \text{mW cm}^{-2}$ of UV illumination for 1 min to crosslink the hole-transport layer.

For the emissive layer, $\text{Ir}(\text{ppy})_3$ or $\text{Ir}(\text{pppy})_3$ (6 or 12 wt%) was mixed with the host material, and all materials dissolved in chlorobenzene (1 mL, 99.8% purity, distilled and then oxygenated). 40–50 nm thick films were then spin coated (60 s at 1000 rpm, acceleration $10\ 000\ \text{rpm s}^{-1}$) onto the UV-crosslinked poly-TPD-F layer. After spin-coating, the samples were baked at $75\text{ }^{\circ}\text{C}$ for 15 min. Chlorobenzene was then used to remove the emissive layer in the area not covered by poly-TPD-F, exposing the ITO substrate to provide electrical contact to the anode. The samples were then transferred, under a N_2 atmosphere, into a SPECTROS (Kurt J. Lesker) thermal-deposition system directly connected to the wet-glove box.

For the hole-blocking/electron-transport layer, a 40 nm thick BCP layer was vacuum deposited at a pressure below 2×10^{-7} Torr and a rate of $0.4\ \text{\AA s}^{-1}$. Then, a 2.4 nm layer of lithium fluoride (LiF), as an electron-injection layer, and a 200 nm-thick

aluminum cathode were vacuum deposited through a shadow mask at a pressure below 3×10^{-7} Torr and at rates of 0.15 \AA s^{-1} and 2 \AA s^{-1} , respectively. The shadow mask used for the evaporation of the metal electrodes yields five devices with an area of *ca.* 0.1 cm^2 per substrate. The device testing was performed in an inert atmosphere and without exposing the devices to air immediately following the deposition of the metal cathode.

Blue-emitting devices were fabricated in an analogous fashion, except: the ITO was treated with pentafluorobenzylphosphonic acid (PFBPA)¹⁴ as previously described¹⁵ prior to depositing the hole-transport material; Sty₂-TCz (see Fig. 1 for structure, ESI† for synthesis) was used as the hole-transport material in place of poly-TPD-F; Firpic was used as the emitter; and crosslinking was carried out by heating to 200 °C for 30 min.

Synthesis of polymeric host materials

The synthesis of monomers **1** and **2** are given in the ESI.†

Poly-1. A solution of 1st generation Grubbs catalyst (0.0290 g, 0.035 mmol) in dry CH₂Cl₂ (5 mL) was added dropwise to a solution of **1** (2.5401 g, 3.85 mmol) in dry CH₂Cl₂ (15 mL) under nitrogen. After 40 min the reaction was quenched by vinyl ethyl ether (1.0 mL). Then the reaction mixture was added dropwise to rapidly stirred methanol (400 mL) to precipitate the polymer. The crude product was redissolved in dichloromethane (10 mL) and then reprecipitated into acetone (400 mL); this process was repeated twice, but using methanol (400 mL) in place of acetone, and the precipitate dried to give an off-white solid (2.258 g, 89%). ¹H NMR (400 MHz, CDCl₃): δ 8.08 (m, br, 2H), 8.02 (m, br, 4H), 7.45 (m, br, 4H), 7.24 (m, br, 8H), 7.14 (m, br, 4H), 5.11 (m, br, 2H), 4.16 (m, br, 2H), 2.70–1.75 (m, br, 7H), 1.24–0.93 (m, br, 8H). Anal. calcd for C₄₈H₄₁N₃: C, 87.37; H, 6.26; N, 6.37. Found: C, 86.84; H, 6.23; N, 6.38%.

Poly-2. A solution of 1st generation Grubbs initiator (0.0339 g, 0.041 mmol) in dry CH₂Cl₂ (5 mL) was added dropwise to a stirred solution of **2** (2.5406 g, 4.23 mmol) in CH₂Cl₂ (15 mL) under nitrogen. After 40 min the reaction was quenched by the additional of vinyl ethyl ether (1.0 mL). The reaction mixture was then added dropwise to rapidly stirred methanol (400 mL) to precipitate the polymer. The crude product was redissolved in dichloromethane (10 mL) and then reprecipitated into acetone (400 mL); this process was repeated twice, but using methanol (400 mL) in place of acetone, and the precipitate was dried to give an off-white solid (2.324 g, 92%). ¹H NMR (400 MHz, CDCl₃): δ 8.69 (m, br, 1H), 8.19 (m, br, 2H), 8.00 (m, br, 2H), 7.59–7.49 (m, br, 5H), 7.33 (m, br, 1H), 6.98 (m, br, 1H), 5.26 (m, br, 2H), 3.96 (m, br, 2H), 2.91–1.73 (m, br, 6H), 1.59–0.86 (m, br, 18H). Anal. calcd for C₃₈H₄₀N₄O₃: C, 75.97; H, 6.71; N, 9.33; Found: C, 75.91; H, 6.69; N, 9.34%.

Poly-1-co-2. A solution of the 1st generation Grubbs initiator (0.0062 g, 0.0075 mmol) in dry CH₂Cl₂ (4 mL) was added dropwise to a solution of **1** (0.4956 g, 0.752 mmol) and **2** (0.4549 g, 0.757 mmol) in dry CH₂Cl₂ (8 mL). After 4 h the reaction appeared complete according to TLC and was quenched with vinyl ethyl ether (0.5 mL). Then the reaction mixture was added dropwise to rapidly stirred methanol (200 mL) to precipitate the

polymer. The crude product was redissolved in dichloromethane (3 mL) and then reprecipitated into methanol (200 mL) three times and dried to give an off-white solid (0.775 g, 82%). ¹H NMR (400 MHz, CDCl₃): δ 8.69 (m, br, 1H), 8.12 (m, br, 4H), 8.03 (m, br, 6H), 7.50 (m, br, 9H), 7.27 (m, br, 8H), 7.15 (m, br, 5H), 6.98 (m, br, 1H), 5.18 (m, br, 4H), 4.31 (m, br, 2H), 3.89 (m, br, 2H), 2.83–1.53 (m, br, 14H), 1.48–1.04 (m, br, 25H). Anal. calcd for C₈₆H₈₁N₇O₃: C, 81.94; H, 6.48; N, 7.78. Found: C, 81.94; H, 6.29; N, 7.67%.

Poly-1-b-2. A solution of the 1st generation Grubbs initiator (0.0035 g, 0.0042 mmol) in dry CH₂Cl₂ (2 mL) was added dropwise to a solution of **2** (0.2726 g, 0.454 mmol) in dry CH₂Cl₂ (4 mL) under nitrogen. After 30 min the reaction appeared complete by TLC and the reaction mixture (6 mL) was added to the second monomer **1** (0.3055 g, 0.463 mmol). After 30 min the polymerization was quenched with vinyl ethyl ether (0.2 mL). Then the reaction mixture was added dropwise to rapidly stirred acetone (200 mL) to precipitate the polymer. The crude product was redissolved in CH₂Cl₂ (3 mL) and then reprecipitated from acetone 200 mL; this process was repeated twice, but using methanol (200 mL) in place of acetone, and the precipitate was dried to give an off-white solid (0.454 g, 79%). ¹H NMR (400 MHz, CDCl₃): δ 8.69 (m, br, 1H), 8.19–8.01 (m, br, 11H), 7.60–7.24 (m, br, 13H), 7.13–6.98 (m, br, 9H), 5.27 (m, br, 2H), 5.11 (m, br, 2H), 4.14 (m, br, 2H), 3.95 (m, br, 2H), 2.88–2.15 (m, br, 5H), 1.82–1.75 (m, br, 9H), 1.40–0.88 (m, br, 25H). Anal. calcd for C₈₆H₈₁N₇O₃: C, 81.94; H, 6.48; N, 7.78. Found: C, 82.20; H, 6.43; N, 7.67%.

Results and discussion

Synthesis and thermal characterization

We chose to use norbornene side-chains due to the potentially living nature of ring-opening metathesis polymerization (ROMP),¹⁶ which we anticipated would enable homo- and copolymers to be synthesized with similar molecular weights and would permit the synthesis of well-defined diblock copolymers. The triscarbazole and *m*-bis(diaryloxadiazole)benzene side chains were chosen since in our previous work¹⁰ a blend of polymers containing these moieties was successfully used as polymer blend host for green phosphorescent emitters. A long flexible spacer was introduced between the host moieties and the polymerizable group in an attempt to reduce any influence of the side chain on the polymerization rate of the monomer and hence our ability to obtain random copolymers. As shown in Scheme 1, monomers **1** and **2** were synthesized by nucleophilic substitution reactions of 5-(5-bromopentyl)-norbornene (*ca.* 17 : 3 *endo* : *exo* isomer mixture) with triscarbazole and a hydroxyl-functionalized *m*-bis(diaryloxadiazole)benzene, which was, in turn, obtained through a multi-step synthesis (see ESI† for details), respectively. The homopolymers, poly-**1** and poly-**2**, and two copolymers, poly-**1-co-2** and poly-**1-b-2**, were synthesized using 1 mol% of the “first-generation” Grubbs initiator in dichloromethane under nitrogen atmosphere at room temperature. The polymers were purified by repeated dissolution-precipitation processes. All polymers were characterized by ¹H NMR spectroscopy, gel-permeation chromatography (GPC),

and elemental analysis. The number- and weight-average molecular weights (M_n and M_w respectively) and the polydispersity indices ($PDI = M_w/M_n$) are shown in Table 1. The PDIs range from 1.5 to 1.6 and the average degrees of polymerization range from approximately 30 to 60. The decomposition temperatures (T_d) and the glass-transition temperatures (T_g) were measured under nitrogen by thermal gravimetric analysis (TGA) and differential scanning calorimetry (DSC), respectively, and are also summarized in Table 1: all polymers possess relatively high T_d values in the vicinity of 400 °C. The glass-transition temperature of poly-1 (120 °C) is much lower than that of poly-2 (206 °C), consistent with the fused aromatic rings of the triscarbazole moieties leading to a less flexible structure than in the oxadiazole material, where five aromatic rings are connected by single bonds in a linear fashion. The glass-transition temperatures of both copolymers and of a 1 : 1 poly-1/poly-2 blend are intermediate between those of the two homopolymers; however, while poly-1-co-2 shows a comparably sharp glass transition to the homopolymers, those for the block copolymer and the physical blends are considerably broader.

Optical properties

The absorption and emission spectra of the polymers (Fig. 2, Table S2, ESI†) were measured in dilute CH_2Cl_2 solution at room temperature. The absorption and emission of these polymers with oxadiazole/triscarbazole side chains are similar to those of previously reported materials containing similar structural motifs.^{10,17} As shown in Fig. 2, the absorption spectra of both random and block copolymers are very similar to the spectrum of a 1 : 1 blend of the homopolymers, which in turn is essentially the sum of the spectra of the unblended homopolymers, indicating very little ground-state interaction between the triscarbazole and oxadiazole moieties in the copolymers. The emission spectrum of the block copolymer is also similar to that of the blend in showing features characteristic of both triscarbazole and bis(oxadiazolyl)benzene motifs. That of the random polymer is qualitatively different, firstly in that the oxadiazole-based emission is much weaker than that from the triscarbazole moiety, suggesting significant oxadiazole-to-triscarbazole energy transfer, as expected if the two groups are indeed randomly distributed in the polymer, and secondly, in showing an additional broad emission with a maximum at *ca.* 475 nm (2.6 eV). This is tentatively attributed to emission from a

charge-transfer complex or exciplex formed between the oxadiazole acceptor and triscarbazole donor side chains. The poor overlap between emission from the low-lying state and the absorption spectrum of $\text{Ir}(\text{ppy})_3$ (onset of absorption = *ca.* 500 nm) may impair the efficiency of singlet-energy transfer to this phosphor; moreover, this state may be accompanied by an even lower lying triplet charge-transfer state, also affecting triplet-energy transfer ($\text{Ir}(\text{ppy})_3$ adiabatic triplet energy = 2.4 eV¹⁸). The absorption and emission spectra of spin-coated films of the polymers were also measured at room temperature and are shown in Fig. 3. Oxadiazole-to-triscarbazole energy transfer appears to be more significant for films of the copolymers and blends than in solution. The separate low-energy feature seen in solution for the random copolymer and attributed to a charge-transfer state is not discernable in the film spectrum; however, the changes observed between thin-film emission spectra of poly-1, the blend, poly-1-*b*-2, and poly-1-*co*-2 are consistent with increasing contributions from a feature at low energy relative to that from the triscarbazole moieties, also consistent with a possible charge-transfer state.

OLED performance

A series of green-emitting OLEDs were fabricated using poly-1-*co*-2, poly-1-*b*-2, and a 1 : 1 poly-1/poly-2 blend as hosts for $\text{Ir}(\text{ppy})_3$. The general device structure of the OLEDs was indium tin oxide (ITO)/poly-TPD-F (35 nm)/host: $\text{Ir}(\text{ppy})_3$ (6 or 12 wt%) (40 nm)/BCP (40 nm)/LiF/Al. Poly-TPD-F¹³ (Fig. 1), which we have used extensively in previous work,¹⁹ was used as a photocrosslinkable hole transporting material, and 2,9-dimethyl-4,7-diphenyl-1,10-phenanthroline, BCP (Fig. 1), was used as the electron-transport material. The performance of the OLEDs is summarized in Table 2, along with that of green- and blue-emitting devices with the structures ITO/poly-TPD-F (35 nm)/host: $\text{Ir}(\text{ppy})_3$ (6 wt%) (40 nm)/BCP (40 nm)/LiF/Al and ITO/PFBPA/Sty₂-TCz (35 nm)/host:FIrpic (6 wt%) (40 nm)/BCP (40 nm)/LiF/Al, respectively.

All of the $\text{Ir}(\text{ppy})_3$ devices gave the characteristic green emission of phosphorescent guests and possessed turn-on voltages lower than 8.5 V. Although, as discussed above, the random and block copolymers show rather different emission properties in solution and, to a lesser extent, in films, their performance as hosts in OLEDs is quite similar (entries 1 and 2 vs. 3 and 4), with their relative efficiency depending on the phosphor loading. In previous work, more significant differences in EQE were observed between block and random copolymers with triphenylamine and diaryloxadiazole side chains as hosts for either (tpy)₂Iracac or FPt in single-layer OLEDs, with much higher EQEs being seen for the block polymers.²⁰ The present devices based on the 1 : 1 blend of polymers (entries 5 and 6), particularly those employing a lower phosphor loading, exhibit significantly higher EQEs than the corresponding random (entries 1 and 2) or block copolymer devices (entries 3 and 4). The maximum EQE of 16.8% observed for the 6 wt% $\text{Ir}(\text{ppy})_3$ blend (entry 5) is considerably higher than the corresponding values reported for analogous devices using 1 : 1.1 w/w PVK/I mixtures as hosts (9.6–10.1%, values that are

Table 1 GPC and thermal data

Polymer	M_w^a /kDa	M_n^a /kDa	PDI	T_d^b /°C	T_g^c /°C
Poly-1	35	23	1.5	445	206
Poly-2	58	36	1.6	397	120
Poly-1- <i>co</i> -2	74	47	1.6	423	154
Poly-1- <i>b</i> -2	62	38	1.6	410	144
1 : 1 poly-1/poly-2	n/a	n/a	n/a	405	136

^a Molecular weights estimated by GPC calibrated by polystyrene standards. ^b Measured by TGA, defined at temperature at which 5% mass loss is seen at a heating rate of 20 °C min⁻¹. ^c Measured by DSC at a heating rate of 10 °C min⁻¹.

Table 2 Performance of OLEDs with triscarbazole/*m*-bis(diaryloxadiazole)benzene polymer hosts

Entry	Polymeric host	Wt% guest	$V_{\text{turn-on}}$ (10 cd m ⁻²)/V	EQE (%) at 100 cd m ⁻²	Max. EQE (%)	Max. current efficacy/cd A ⁻¹	Max. power efficacy/ lm W ⁻¹
1	Poly-1- <i>co</i> -2	6% Ir(ppy) ₃	7.4	6.0	6.2	23	8.6
2	Poly-1- <i>co</i> -2	12% Ir(ppy) ₃	8.5	6.7	7.5	28	9.7
3	Poly-1- <i>b</i> -2	6% Ir(ppy) ₃	7.2	6.8	7.2	17	6.3
4	Poly-1- <i>b</i> -2	12% Ir(ppy) ₃	6.6	5.5	6.6	16	6.7
5	1 : 1 poly-1/poly-2	6% Ir(ppy) ₃	8.0	15.9	16.8	34	10
6	1 : 1 poly-1/poly-2	12% Ir(ppy) ₃	6.0	9.0	9.4	35	13
7	1 : 1.5 poly-1/poly-2	6% Ir(pppy) ₃	6.5	16.4	17.2	50	22
8	1.5 : 1 poly-1/poly-2	6% Ir(pppy) ₃	6.0	21.0	28.0	66	31
9	1 : 1 poly-1/poly-2	6% FIrpic	8.0	2.5	2.9	9.9	2.8
10	1 : 1.5 poly-1/poly-2	6% FIrpic	9.2	1.4	1.4	5.0	1.4
11	1.5 : 1 poly-1/poly-2	6% FIrpic	8.2	2.9	3.7	12.7	3.3

still higher than those obtained in the present study using copolymers),^{6c} although the turn-on voltage is a little higher in the present devices and the current efficacy is only a little higher.

It has previously been suggested that random or diblock copolymer ambipolar host systems might be expected to perform better than analogous homopolymer blends, given the possibility of obtaining macroscopic (μm -scale) phase separation in the latter.²⁰ One contributor to our observation of *higher* efficiencies in the *blend*-based devices may be a less significant loss of excitons to low-lying triscarbazole/oxadiazole charge-transfer-type states (see discussion of emission spectra above). These charge-transfer states presumably require donor/acceptor proximity and so will be suppressed to some extent by any donor/acceptor segregation, raising the question of the length scale over which such separation might occur. Accordingly, we examine the microstructure of poly-1/poly-2 blends in the following section.

Entries 7 and 8 in the table demonstrate that even more efficient devices can be obtained with poly-1/poly-2 host blends by using Ir(pppy)₃ in place of Ir(ppy)₃ as the phosphorescent emitter. This is consistent with our previous observations using PVK/I blends, where an increase in the maximum EQE from 10.1 to 13.6% was seen on replacing Ir(ppy)₃ with Ir(pppy)₃ and was attributed to reduced aggregation and improved miscibility with the host polymers of the bulkier phosphorescent guest.^{6c} The present devices are significantly more efficient than analogous Ir(pppy)₃ device in which the host is a PVK/I blend,^{6c} or devices using a different hole-transport layer and a II/III blend as host.¹⁰ Indeed, the efficiency of 21% (at 100 cd cm⁻²) obtained for 1.5 : 1 poly-1/poly-2 approaches the highest value reported to date for a green PHOLEDs with a solution-processed emissive layer (23.8% at 1000 cd m⁻²).²¹

Entries 9–11 in Table 2 refer to devices in which a thermally cross-linkable triscarbazole derivative, Sty₂-TCz, was used in place of poly-TPD-F,²² the ITO was pretreated with pentafluorobenzylphosphonic acid to facilitate effective wetting by Sty₂-TCz, and the greenish-blue emitter FIrpic was used, and thus demonstrate that this polymer-blend host

approach can also be successfully applied to blue-emitting devices.

Microstructure of the host films

Differences in domain size and shapes in polymer blends and in block copolymers can potentially affect OLED performance in a variety of ways,¹⁸ influencing charge transport, charge recombination, and, depending on the location of the phosphors relative to the charge-recombination sites, the efficiency of energy transfer to the phosphor. To investigate the microstructures of poly-1-*b*-2 and a 1 : 1 poly-1/poly-2 blend, we investigated films of the materials using DSC and solid-state NMR. As discussed and shown above (Fig. 4) the thermal behavior of the 1 : 1 poly-1/poly-2 blend is similar to that of poly-1-*b*-2; in contrast to the homopolymers and the random copolymers, which possess a well-defined glass transitions, these materials exhibit a much broader less-well-defined glass transition, potentially indicating a range of different local environments in these films. However, there is no evidence of macro-scale phase separation of the two homopolymers in the blend, which would be expected to result in observation of two separate glass transitions.

Solid-state ¹H spin-diffusion experiments can potentially yield more quantitative information about the domain size and geometry in multicomponent systems.^{12,23} The principle is illustrated in Fig. 5a. For a two-domain system, the first step of the ¹H spin diffusion experiments is to selectively remove the magnetization of one domain through a suitable sequence of rf-pulses, leaving that of the other phase unaffected due to differences in either the chemical shifts or the conformational mobility between two domains. The remaining magnetization will then be transferred throughout the sample *via* the network of the dipolar couplings between ¹H nuclei in both phases and the magnetization of either domain will be recorded as a function of time. Using the ¹H spin diffusion coefficients for each domain (which are usually deduced from spin-spin relaxation experiments), the ¹H spin diffusion can be simulated by solving Fick's diffusion equations (see Experimental section) for a given domain size and geometry. By fitting the simulated time dependence of the magnetization intensity with the

experimental results, the approximate domain size and geometry can be determined.

In our experiments, the selective magnetization was achieved through the difference in conformational mobility between the oxadiazole and triscarbazole side chains at 190 °C, as revealed by spin-spin relaxation measurements at the same temperature, which showed two distinct relaxation times from the mobile and rigid domains respectively (see ESI†). The magnetization of the mobile domain, assumed to be the oxadiazole domain based on the observation of a lower glass-transition temperature for the corresponding homopolymer than for the triscarbazole homopolymer, was then selected through the dipolar filter for the spin-diffusion experiments and the amount of this magnetization was observed as a function of a mixing time, providing insight into the timescale at which magnetization is transported out of this domain into the triscarbazole domain. The experimental and the best-fit simulated curves of the temporal evolution of the normalized magnetization in the oxadiazole domain for the 1 : 1 poly-1/poly-2 blend and for poly-1-*b*-2 are summarized in Fig. 5b. The normalized intensities for both samples equilibrate at values of *ca.* 0.5, consistent with oxadiazole and triscarbazole moieties being present in a 1 : 1 ratio in both cases and having comparable ¹H concentrations. The blend shows a significantly larger characteristic time for the ¹H spin diffusion than the block polymer, which implies that larger domains are present in the physical blend sample. Using the spin-diffusion coefficients for the oxadiazole and triscarbazole domains in the two materials obtained from spin-spin relaxation experiments (see ESI†), the ¹H spin diffusion processes for these two samples were simulated (as described in the Experimental section) to obtain information about the domain geometry and the characteristic lengths. The data for the diblock copolymer were successfully simulated using a layered structure with one-dimensional spin-transport characteristics (characteristic length = 1.8 nm), whereas the blend data were fitted using a cubic structure with three-dimensional spin-transport (characteristic length = 16.4 nm).

It should be noted the obtained domain geometry and sizes may not represent the exact domain dimensions; microstructures in polymeric materials are usually irregular, ill-defined, and locally dependent. Moreover, without a detailed knowledge of the location of the phosphor molecules within the polymers, or of the orientation of the layered structures modeled for the block polymer, the NMR data do not fully explain the differences in OLED performance. However, the spin-diffusion results clearly suggest qualitative differences in the nanoscale structure of the two samples. These differences in domain sizes are broadly consistent with our tentative assignment (see above) of differences in the emission spectra of films of the block copolymer and the blend to the decreased contribution of charge-transfer-type emission in the latter case. Furthermore, the spin-diffusion data for the blend are consistent with the inference of the absence of macroscopic phase separation from the DSC data.

Conclusion

Random and block copolymers of triscarbazole- and bis-(oxadiazole)benzene-functionalized norbornene monomers have been compared as solution-processed ambipolar hosts for Ir(ppy)₃ in green-emitting OLEDs to a blend of the corresponding homopolymers. The blend-based OLEDs exhibit considerably higher external quantum efficiencies than the diblock and random copolymer devices. DSC and solid-state NMR experiments indicate that the blend does not undergo macroscopic phase segregation, but exhibits a nanoscale separation, which is characterized by a different domain dimensionality and size to that observed for the block polymer. The blend approach has led to some of the most efficient green-phosphorescent OLEDs with solution-processed emissive layers reported to date.

Acknowledgements

Support from Solvay S.A. and the Science and Technology Center Program of the National Science Foundation (DMR-0120967) is gratefully acknowledged.

Notes and references

- (a) M. A. Baldo, D. F. O'Brien, Y. You, A. Shoustikov, S. Sibley, M. E. Thompson and S. R. Forrest, *Nature*, 1998, **395**, 151; (b) Y. Kawamura, K. Goushi, J. Brooks, J. J. Brown, H. Sasabe and C. Adachi, *Appl. Phys. Lett.*, 2005, **86**, 071104.
- M. A. Baldo, C. Adachi and S. R. Forrest, *Phys. Rev. B: Condens. Matter Mater. Phys.*, 2000, **62**, 10967.
- (a) N. C. Giebink and S. R. Forrest, *Phys. Rev. B: Condens. Matter Mater. Phys.*, 2008, **77**, 235215; (b) S. H. Kim, J. Jang, K. S. Yook and J. Y. Lee, *Appl. Phys. Lett.*, 2008, **92**, 023513.
- (a) C. Adachi, R. C. Kwong and S. Forrest, *Org. Electron.*, 2001, **2**, 37; (b) S. Lamansky, P. I. Djurovich, F. Abdel-Razzaq, S. Garon, D. L. Murphy and M. E. Thompson, *J. Appl. Phys.*, 2002, **92**, 1570; (c) X. Gong, J. C. Ostrowski, D. Moses, G. C. Bazan and A. J. Heeger, *Adv. Funct. Mater.*, 2003, **13**, 439; (d) X. H. Yang and D. Neher, *Appl. Phys. Lett.*, 2004, **84**, 2476; (e) X. H. Yang, F. Jaiser, S. Klinger and D. Neher, *Appl. Phys. Lett.*, 2006, **88**, 021107.
- A. Chaskar, H.-F. Chen and K.-T. Wong, *Adv. Mater.*, 2011, **23**, 3876.
- (a) X. H. Yang, D. C. Muller, D. Neher and K. Meerholz, *Adv. Mater.*, 2006, **18**, 948; (b) K. Zhang, Z. Chen, C. L. Yang, X. W. Zhang, Y. T. Tao, L. Duan, L. Chen, L. Zhu, J. G. Qin and Y. Cao, *J. Mater. Chem.*, 2007, **17**, 3451; (c) S. J. Kim, Y. D. Zhang, C. Zuniga, S. Barlow, S. R. Marder and B. Kippelen, *Org. Electron.*, 2011, **12**, 492.
- L. Deng, P. T. Furuta, S. Garon, J. Li, D. Kavulak, M. E. Thompson and J. M. J. Frechet, *Chem. Mater.*, 2006, **18**, 386.
- K. Zhang, Y. Tao, C. Yang, H. You, Y. Zou, J. Qin and D. Ma, *Chem. Mater.*, 2008, **20**, 7324.
- (a) K. Brunner, A. van Dijken, H. Borner, J. J. Bastiaansen, N. M. Kiggen and B. M. Langeveld, *J. Am. Chem. Soc.*, 2004,

- 126, 6035; (b) M. Guan, Z. Q. Chen, Z. Q. Bian, Z. W. Liu, Z. L. Gong, W. Baik, H. J. Lee and C. H. Huang, *Org. Electron.*, 2006, **7**, 330; (c) M. K. Leung, C. C. Yang, J. H. Lee, H. H. Tsai, C. F. Lin, C. Y. Huang, Y. O. Su and C. F. Chiu, *Org. Lett.*, 2007, **9**, 235; (d) Y. Tao, Q. Wang, C. Yang, Q. Wang, Z. Zhang, T. Zou, J. Qin and D. Ma, *Angew. Chem., Int. Ed.*, 2008, **47**, 8104; (e) Y. Tao, Q. Wang, C. Yang, C. Zhong, K. Zhang, J. Qin and D. Ma, *Adv. Funct. Mater.*, 2010, **20**, 304; (f) Y. Zhang, W. Haske, D. Cai, S. Barlow, B. Kippelen and S. R. Marder, *RSC Adv.*, 2013, **3**, 23514.
- 10 C. A. Zuniga, J. Abdallah, W. Haske, Y. D. Zhang, I. Coropceanu, S. Barlow, B. Kippelen and S. R. Marder, *Adv. Mater.*, 2013, **25**, 1739.
- 11 F. Mellinger, M. Wilhelm and H. W. Spiess, *Macromolecules*, 1999, **32**, 4686.
- 12 J. Clauss, K. Schmidt-Rohr and H. W. Spiess, *Acta Polym.*, 1993, **44**, 1.
- 13 (a) R. D. Hreha, Y. D. Zhang, B. Domercq, N. Larriveau, J. N. Haddock, B. Kippelen and S. R. Marder, *Synthesis*, 2002, 1201; (b) B. Domercq, R. D. Hreha, Y.-D. Zhang, N. Larriveau, J. N. Haddock, C. Schultz, S. R. Marder and B. Kippelen, *Chem. Mater.*, 2003, **15**, 1491.
- 14 P. Kim, S. C. Jones, P. J. Hotchkiss, J. N. Haddock, B. Kippelen, S. R. Marder and J. W. Perry, *Adv. Mater.*, 2007, **19**, 1001.
- 15 A. Sharma, P. J. Hotchkiss, S. R. Marder and B. Kippelen, *J. Appl. Phys.*, 2009, **105**, 084507.
- 16 (a) W. J. Feast, *Makromol. Chem., Macromol. Symp.*, 1992, **53**, 317; (b) R. H. Grubbs, S. J. Miller and G. C. Fu, *Acc. Chem. Res.*, 1995, **28**, 446; (c) R. R. Schrock, *Top. Organomet. Chem.*, 1998, **1**, 1.
- 17 (a) P. Zhang, B. Xia, Q. Zhang, B. Yang, M. Li, G. Zhang and W. Tian, *Synth. Met.*, 2006, **156**, 705; (b) S. Zhang, R. Chen, J. Yin, F. Liu, H. Jiang, N. Shi, Z. An, C. Ma, B. Liu and W. Huang, *Org. Lett.*, 2010, **12**, 3438.
- 18 M. A. Baldo and S. Forrest, *Phys. Rev. B: Condens. Matter Mater. Phys.*, 2000, **62**, 10958.
- 19 For example, (a) A. Haldi, A. Kimyonok, B. Domercq, L. E. Hayden, S. C. Jones, S. R. Marder, M. Weck and B. Kippelen, *Adv. Funct. Mater.*, 2008, **18**, 3056; (b) X. W. Zhan, A. Haldi, J. S. Yu, T. Kondo, B. Domercq, J. Y. Cho, S. Barlow, B. Kippelen and S. R. Marder, *Polymer*, 2009, **50**, 397; (c) Y. Zhang, C. Zuniga, S.-J. Kim, D. Cai, S. Barlow, S. Salman, V. Coropceanu, J.-L. Brédas, B. Kippelen and S. Marder, *Chem. Mater.*, 2011, **23**, 4002.
- 20 B. Ma, B. J. Kim, L. Deng, D. A. Poulsen, M. E. Thompson and J. M. J. Frechet, *Macromolecules*, 2007, **40**, 8156.
- 21 J.-H. Jou, C.-J. Li, S.-M. Shen, S.-H. Peng, Y.-L. Chen, Y.-C. Jou, J. H. Hong, C.-L. Chin, J.-J. Shyue, S.-P. Chen, J.-Y. Li, P.-H. Wang and C.-C. Chen, *J. Mater. Chem.*, 2013, **1**, 4201.
- 22 Chosen because triscarbazole derivatives have been found to have higher triplet energies (2.9 eV, M.-H. Tsai, Y.-H. Hong, C.-H. Chang, H.-C. Su, C.-C. Wu, A. Matoliukstyte, J. Simokaitiene, S. Grigalevicius, J. V. Grazulevicius and C.-P. Hsu, *Adv. Mater.*, 2007, **19**, 862) than TPD derivatives (2.3 eV, ref. 18), reducing the possibility of triplet energy transfer from Firpic (triplet energy = 2.6 eV, C. Adachi, R. Kwong, P. I. Djurovich, V. Adamovich, M. Baldo, M. E. Thompson and S. Forrest, *Appl. Phys. Lett.*, 2001, **79**, 2082) to the hole-transport layer. It may be possible to improve the performance of the blue-emitting devices further by replacing the BCP (triplet energy = 2.5 eV, ref. 18) with an electron-transport material having a higher triplet energy.
- 23 (a) M. Mauri, Y. Thomann, H. Schneider and K. Saalwachter, *Solid State Nucl. Magn. Reson.*, 2008, **34**, 125; (b) R. C. Nieuwendaal, H. W. Ro, D. S. Germack, R. J. Kline, M. F. Toney, C. K. Chan, A. Agrawal, D. Gundlach, D. L. VanderHart and D. M. DeLongchamp, *Adv. Funct. Mater.*, 2012, **22**, 1255.